BI-LEVEL TENSOR DECOMPOSITION FOR HYPERSPECTRAL IMAGE RESTORATION

Yun-Yang Liu[a, d], Xi-Le Zhao[a,], Jin-Yu Xie[b], Zhi Xu [c], Gemine Vivone[d]*

[a]School of Mathematical Sciences, University of Electronic Science and Technology of China, Chengdu, 611731, China
[b]Yingcai Honors College, University of Electronic Science and Technology of China, Chengdu, 611731, China
[c]School of Mathematics and Statistics, Taiyuan Normal University, Jinzhong, 030619, China
[d]Institute of Methodologies for Environmental Analysis, National Research Council, Tito Scalo, 85050, Italy

ABSTRACT

This paper proposes a bi-level tensor decomposition (BLTD), properly exploiting the characterization advantages of tensor subspace representation (TSR) and tensor ring decomposition (TRD). More specifically, the first level is related to the decomposition of a third-order tensor into its TSR using the tensor-tensor product (t-product), and the second level performs TRD on the coefficient tensor obtained by TSR. Leveraging the proposed BLTD, we design a bi-level tensor nuclear norm (BLTNN)-based model for hyperspectral images (HSIs) denoising. To solve the model, we develop an efficient alternating direction method of multipliers (ADMM)-based algorithm. Experimental results demonstrate the superior performance of our method compared to existing methods.

Index Terms— Hyperspectral image restoration, bi-level tensor decomposition, low-rankness

1. INTRODUCTION

Hyperspectral images (HSIs) contain abundant spatial-spectral information and are valuable in many applications [1]. However, because of the complex observation environments and limitations in imaging systems, HSIs are frequently corrupted by different types of noise, such as Gaussian noise, salt-and-pepper noise, and stripes. These noises affect the quality of HSIs and also the accuracy of downstream applications. Therefore, HSI denoising is crucial for ensuring the effectiveness of subsequent applications.

Many HSI denoising methods rely on the low-rank prior because of its ability to preserve the global structure of the data, leading to promising performance. Regarding the low-rank matrix-based restoration methods, Zhang *et al.* proposed a classical low-rank matrix recovery (LRMR)-based model for HSI denoising [2]. Considering that the noise intensity in different bands is different, He *et al.* developed a patch-wise low-rank matrix approximation (LRMA)-based method to effectively remove the mixed noise [3]. Nevertheless, the majority of matrix-based methods unfold the HSI cube into a matrix, resulting in the loss of intrinsic information within the cube. Hence, numerous low-rank tensor-based restoration methods have been proposed. Renard *et al.* introduced a HSI denoising model using low-rank tensor approximation (LRTA) based on Tucker decomposition [4]. Fan *et al.* developed a model for HSI denoising based on low-tubal-rank tensor recovery (LRTR), where tubal-rank is defined from tensor singular value decomposition (t-SVD) [5]. By generalizing the t-SVD to mode-k t-SVD, Zheng *et al.* proposed tensor fibered-rank and its convex relaxation, i.e., three-directional tensor nuclear norm (3DTNN), for HSI denoising [6].

In the framework of (mode-k) t-SVD, low-tubal-rank decomposition and low-fibered-rank decomposition indicate that the HSI has low-rank tensor subspace representation (TSR) along the third-mode and all three modes, respectively. However, they only exploit a single-level low-rankness of the data and ignore the underlying low-rankness of the coefficient

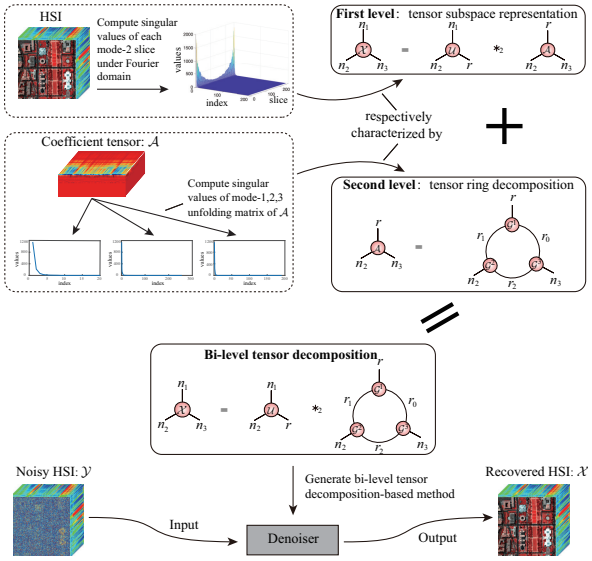

Fig. 1. BLTD-based method for HSI denoising.

*This research is supported by NSFC (No. 12371456, 62131005, and 12171072), Sichuan Science and Technology Program (No. 2023ZYD0007), Fund of Hubei Key Laboratory of Inland Shipping Technology (No. NHHY2023003), National Key Research and Development Program of China (No. 2020YFA0714001). Corresponding author: xlzhao122003@163.com.

tensor obtained by the TSR, as shown in Fig. 1. Therefore, we propose a bi-level tensor decomposition to more accurately characterize the bi-level low-rank structure of the data.

The contribution of this paper is three-fold: i) a novel bi-level tensor decomposition (BLTD), by combining TSR and tensor ring decomposition (TRD) (as in Fig. 1), is proposed; ii) to efficiently remove the mixed noise, we propose a bi-level tensor nuclear norm (BLTNN) by employing the tensor ring nuclear norm (TRNN) as convex relaxation of TRD-rank and develop a BLTNN-based model for HSI denoising; iii) we introduce an alternating direction method of multipliers (ADMM)-based algorithm [7] to solve the proposed model.

Remark 1 *As shown in [6], the mode-1 and mode-2 fibered-ranks are much smaller than the mode-3 fibered-rank, thus we utilize the TSR along mode-2 in this paper.*

2. PRELIMINARIES

In this section, we mainly introduce the relevant definitions of TSR, TRD [8], and TRNN [9] for subsequent discussion.

For $\mathcal{X} \in \mathbb{R}^{n_1 \times n_2 \times n_3}$, we use x_{ijk} and $\mathbf{X}(i) \in \mathbb{R}^{n_1 \times n_3}$ to denote its (i,j,k)-th element and i-th mode-2/lateral slice, respectively. The ℓ_1 norm and Frobenius norm of $\mathcal{X}$ are defined as $\|\mathcal{X}\|_1 := (\sum_{ijk} |x_{ijk}|)$ and $\|\mathcal{X}\|_F := (\sum_{ijk} x_{ijk}^2)^{1/2}$, respectively. The inner product of $\mathcal{X}$ and $\mathcal{Y}$ is defined as $\langle \mathcal{X}, \mathcal{Y} \rangle := \sum_{ijk} x_{ijk} y_{ijk}$.

Definition 1 (mode-2 t-product) *The mode-2 t-product between $\mathcal{X} \in \mathbb{R}^{n_1 \times n_2 \times n_3}$ and $\mathcal{Y} \in \mathbb{R}^{n_3 \times n_2 \times n_4}$ is defined as*

$$\mathcal{Z} = \mathcal{X} *_2 \mathcal{Y} \Leftrightarrow \mathcal{Z}(i,:,k) = \sum\nolimits_{j=1}^{n_3} \mathcal{X}(i,:,j) \star \mathcal{Y}(j,:,k),$$

where $\mathcal{Z} \in \mathbb{R}^{n_1 \times n_2 \times n_4}$ and $\star$ denotes circular convolution.

Definition 2 (mode-2 conjugate transpose) *The mode-2 conjugate transpose of $\mathcal{X}$, denoted by $\mathcal{X}^{H_2}$, is obtained by conjugate transposing each of the mode-2 slices and then reversing the order of transposed mode-2 slices from 2 to n_2.*

Definition 3 (mode-2 TSR) *The mode-2 TSR of tensor $\mathcal{X} \in \mathbb{R}^{n_1 \times n_2 \times n_3}$ is defined as*

$$\mathcal{X} = \mathcal{U} *_2 \mathcal{A}, \ \text{s.t. } \mathcal{U}^{H_2} *_2 \mathcal{U} = \mathcal{I}_2, \tag{1}$$

where $\mathcal{U} \in \mathbb{R}^{n_1 \times n_2 \times r}$ is a semi-orthogonal basic tensor, $\mathcal{A} \in \mathbb{R}^{r \times n_2 \times n_3}$ is the coefficient tensor, and $\mathcal{I}_2$ is the mode-2 identity tensor where its first mode-2 slice is an identity matrix and the other mode-2 slices are all zeros.

Definition 4 (TRD) *TRD decomposes tensor $\mathcal{X} \in \mathbb{R}^{n_1 \times n_2 \times n_3}$ into a circular multi-linear product over three third-order factor tensors $\mathcal{G}^1 \in \mathbb{R}^{r_0 \times n_1 \times r_1}$, $\mathcal{G}^2 \in \mathbb{R}^{r_1 \times n_2 \times r_2}$, and $\mathcal{G}^3 \in \mathbb{R}^{r_2 \times n_3 \times r_0}$. The element-wise form of TRD can be formulated as*

$$\mathcal{X}(i_1, i_2, i_3) = \mathrm{Tr}(\mathbf{G}^1(i_1)\mathbf{G}^2(i_2)\mathbf{G}^3(i_3)), \tag{2}$$

where $\mathbf{G}^k(i_k)$ denotes the i_k-th lateral slice of $\mathbf{G}^k$, $\mathrm{Tr}(\cdot)$ denotes the matrix trace, and vector (r_0, r_1, r_2) is called TRD-rank. TRD can be simply written as $\mathcal{X} = \Phi(\mathcal{G}^1, \mathcal{G}^2, \mathcal{G}^3)$.

According to the connection of the rank of tensor circular unfolding matrices and the TRD-rank, TRNN is established using a series of tensor circular unfolding matrices.

Definition 5 (TRNN) *Assume tensor $\mathcal{X} \in \mathbb{R}^{n_1 \times n_2 \times n_3}$ with TRD, its TRNN is defined as*

$$\sum\nolimits_{k=1}^{3} \alpha_k \|\mathbf{X}_{<k,d>}\|_*, \tag{3}$$

where $\alpha_k \geq 0$ $(k = 1,2,3)$ with $\sum_{k=1}^{3} \alpha_k = 1$, $\|\cdot\|_*$ denotes the matrix nuclear norm, $d = 1$, $\mathbf{X}_{<k,d>}$ is the circular unfolding matrix of $\mathcal{X}$ satisfying $\mathbf{X}_{<k,d>}(i_t i_{t+1} \cdots i_k, i_{k+1} \cdots i_{t-1}) = \mathcal{X}(i_1, i_2, i_3)$ with

$$t = \begin{cases} k - d + 1, & k \geq d; \\ k - d + 1 + 3, & otherwise, \end{cases} \tag{4}$$

and the corresponding inverse operation is defined as $\mathcal{X} = \mathrm{fold}_k(\mathbf{X}_{<k,d>})$.

3. THE PROPOSED BLTD AND BLTNN

Based on the previous discussion, in this section, we define BLTD and BLTNN.

Firstly, HSIs exhibit significant redundancy in the spectral direction. Thus, we employ TSR to characterize the low-rankness of HSIs in the first level. Secondly, the coefficient tensor in the TSR is also low-rank, as depicted in Fig. 1 where the unfolding matrix along each mode of the coefficient tensor is low-rank. This implies that HSIs have a second-level low-rank structure. To characterize this low-rankness, we employ the TRD. Naturally, the proposed BLTD form is as follows:

Definition 6 (BLTD) *BLTD factorizes tensor $\mathcal{X} \in \mathbb{R}^{n_1 \times n_2 \times n_3}$ into a semi-orthogonal tensor $\mathcal{U} \in \mathbb{R}^{n_1 \times n_2 \times r}$, followed by a circular multi-linear product over three third-order factor tensors $\mathcal{G}^1 \in \mathbb{R}^{r_0 \times r \times r_1}$, $\mathcal{G}^2 \in \mathbb{R}^{r_1 \times n_2 \times r_2}$, and $\mathcal{G}^3 \in \mathbb{R}^{r_2 \times n_3 \times r_0}$, i.e.,*

$$\mathcal{X} = \mathcal{U} *_2 \Phi(\mathcal{G}^1, \mathcal{G}^2, \mathcal{G}^3) \ \text{ s.t. } \mathcal{U}^{H_2} *_2 \mathcal{U} = \mathcal{I}_2, \tag{5}$$

where vector (r, r_0, r_1, r_2) is referred to as the BLTD-rank.

Moreover, we can obtain the convex relaxation of BLTD-rank by substituting the TRD with the TRNN.

Definition 7 (BLTNN) *Assume tensor $\mathcal{X} \in \mathbb{R}^{n_1 \times n_2 \times n_3}$ with BLTD-form, its BLTNN is defined by*

$$\sum\nolimits_{k=1}^{3} \alpha_k \|\mathbf{A}_{<k,d>}\|_*, \tag{6}$$

where $\mathcal{A}$ satisfies $\mathcal{X} = \mathcal{U} *_2 \mathcal{A}$ and $\mathcal{U}^{H_2} *_2 \mathcal{U} = \mathcal{I}_2$, $\mathbf{A}_{<k,d>}$ is the circular unfolding matrix of $\mathcal{A}$.

Algorithm 1 ADMM-based algorithm for the proposed HSI restoration model.

Input: The noisy HSI $\mathcal{Y}$, parameters λ_1, λ_2, r, $\alpha = (\alpha_1, \alpha_2, \alpha_3)$, $\beta = (\beta_1, \beta_2, \beta_3)$, μ, γ, and $\rho = 1.2$.

Initialization: $t = 0$, $\mathcal{X} = \mathcal{Y}, \mathcal{N} = 0, \mathcal{S} = 0, \mathcal{P} = 0, \mathcal{Q} = 0, \mathcal{Z}^k = 0$ $(k = 1, 2, 3)$, $\mathcal{U}$ and $\mathcal{A}$ are obtained by mode-2 truncated t-SVD of $\mathcal{Y}$.

while not converged **do**

Update $(\mathcal{M}^k)^{t+1} = \text{fold}_k \left[D_{\alpha_k/\beta_k} \left(\mathbf{A}^t_{<k,d>} + \frac{1}{\beta_k} (\mathcal{Z}^k)^t_{<k,d>} \right) \right]$, where $D_\tau(\cdot)$ denotes the thresholding SVD operation.

Update $\mathcal{X}^{t+1} = \left(\mu(\mathcal{U}^t *_2 \mathcal{A}^t) - \mathcal{P}^t + \gamma(\mathcal{Y} - \mathcal{N}^t - \mathcal{S}^t) + \mathcal{Q}^t\right)/(\mu + \gamma)$.

Update $\mathcal{N}^{t+1} = (\gamma(\mathcal{Y} - \mathcal{X}^{t+1} - \mathcal{S}^t) + \mathcal{Q}^t)/(2\lambda_1 + \gamma)$.

Update $\mathcal{S}^{t+1} = \text{soft}(\mathcal{Y} - \mathcal{X}^{t+1} - \mathcal{N}^{t+1} + \frac{\mathcal{Q}^t}{\gamma}, \frac{\lambda_2}{\gamma})$, where $\text{soft}(\mathcal{X}, \xi)_{ijs} = \text{sgn}(x_{ijs})\max(|x_{ijs}| - \xi, 0)$.

Update $\mathcal{U}^{t+1} = \hat{\mathcal{V}}^{t+1} *_2 (\hat{\mathcal{U}}^{t+1})^{H_2}$, where $\hat{\mathcal{U}}$ and $\hat{\mathcal{V}}$ are from the t-SVD of $\mathcal{A}^t *_2 (\mathcal{X}^{t+1} + \frac{\mathcal{P}^t}{\mu})^{H_2} = \hat{\mathcal{U}}^{t+1} *_2 \hat{\mathcal{D}}^{t+1} *_2 (\hat{\mathcal{V}}^{t+1})^{H_2}$.

Update $\mathcal{A}^{t+1} = \left(\sum_{k=1}^3 \left(\beta_k (\mathcal{M}^k)^{t+1} - (\mathcal{Z}^k)^t\right) + (\mathcal{U}^{t+1})^{H_2} *_2 (\mu \mathcal{X}^{t+1} + \mathcal{P}^t)\right) / (\sum_{k=1}^3 \beta_k + \mu)$.

Update $\mathcal{P}^{t+1} = \mathcal{P}^t + \mu(\mathcal{X}^{t+1} - \mathcal{U}^{t+1} *_2 \mathcal{A}^{t+1})$; $\mathcal{Q}^{t+1} = \mathcal{Q}^t + \gamma(\mathcal{Y} - \mathcal{X}^{t+1} - \mathcal{N}^{t+1} - \mathcal{S}^{t+1})$; $(\mathcal{Z}^k)^{t+1} = (\mathcal{Z}^k)^t + \beta_k(\mathcal{A}^{t+1} - (\mathcal{M}^k)^{t+1})$, $k = 1, 2, 3$.

Let $\beta = \rho\beta$, $\mu = \rho\mu$, $\gamma = \rho\gamma$.

Check the convergence criterion: $\|\mathcal{X}^{t+1} - \mathcal{X}^t\|_F / \|\mathcal{X}^t\|_F < 10^{-4}$.

end while

Output: The recovered HSI $\mathcal{X}$.

4. THE PROPOSED DENOISING METHOD

Suppose the noise is independent additive noise, the proposed HSI denoising model based on BLTNN is formulated as

$$\begin{aligned} \min_{\mathcal{X},\mathcal{N},\mathcal{S}} \ & \sum_{k=1}^3 \alpha_k \|\mathbf{A}_{<k,d>}\|_* + \lambda_1 \|\mathcal{N}\|_F^2 + \lambda_2 \|\mathcal{S}\|_1, \\ \text{s.t.} \ & \mathcal{Y} = \mathcal{X} + \mathcal{N} + \mathcal{S}, \ \mathcal{X} = \mathcal{U} *_2 \mathcal{A}, \ \mathcal{U}^{\mathrm{H}_2} *_2 \mathcal{U} = \mathcal{I}_2, \end{aligned} \tag{7}$$

where tensors $\mathcal{Y}$ and $\mathcal{X}$ denote the noisy and clean HSIs respectively, $\mathcal{N}$ and $\mathcal{S}$ denote the Gaussian and the sparse noises (including salt-and-pepper noise and stripes), respectively.

We employ the ADMM framework to solve (7). By introducing auxiliary variables $\mathcal{M}^k$ $(k = 1, 2, 3)$, we rewrite (7) as

$$\begin{aligned} \min_{\mathcal{X},\mathcal{N},\mathcal{S}} \ & \sum_{k=1}^3 \alpha_k \|\mathbf{M}^k_{<k,d>}\|_* + \lambda_1 \|\mathcal{N}\|_F^2 + \lambda_2 \|\mathcal{S}\|_1, \\ \text{s.t.} \ & \mathcal{Y} = \mathcal{X} + \mathcal{N} + \mathcal{S}, \ \ \mathcal{A} = \mathcal{M}^k, \ \ k = 1, 2, 3 \\ & \mathcal{X} = \mathcal{U} *_2 \mathcal{A}, \ \ \mathcal{U}^{H_2} *_2 \mathcal{U} = \mathcal{I}_2. \end{aligned} \tag{8}$$

The augmented Lagrangian function of (8) is

$$\begin{aligned} \mathcal{L}(\mathcal{M}^k, \mathcal{X}, \mathcal{N}, \mathcal{S}, \mathcal{U}, \mathcal{A}, \mathcal{P}, \mathcal{Q}, \mathcal{Z}^k) &= \sum_{k=1}^3 \{\alpha_k \|\mathbf{M}^k_{<k,d>}\|_* \\ &+ \langle \mathcal{A} - \mathcal{M}^k, \mathcal{Z}^k \rangle + \frac{\beta_k}{2} \|\mathcal{A} - \mathcal{M}^k\|_F^2\} + \lambda_1 \|\mathcal{N}\|_F^2 \\ &+ \lambda_2 \|\mathcal{S}\|_1 + \langle \mathcal{X} - \mathcal{U} *_2 \mathcal{A}, \mathcal{P} \rangle + \frac{\mu}{2} \|\mathcal{X} - \mathcal{U} *_2 \mathcal{A}\|_F^2 \\ &+ \langle \mathcal{Y} - \mathcal{X} - \mathcal{N} - \mathcal{S}, \mathcal{Q} \rangle + \frac{\gamma}{2} \|\mathcal{Y} - \mathcal{X} - \mathcal{N} - \mathcal{S}\|_F^2, \end{aligned}$$

where $\mathcal{Z}^k$ $(k = 1, 2, 3)$, $\mathcal{P}$, and $\mathcal{Q}$ are the Lagrange multipliers; β_k $(k = 1, 2, 3)$, μ, and γ are the penalty parameters. Within the framework of ADMM, $\mathcal{M}^k$, $\mathcal{X}$, $\mathcal{N}$, $\mathcal{S}$, $\mathcal{U}$, and $\mathcal{A}$ are alternately updated as summarized in Algorithm 1. Moreover, the computational complexity of the proposed algorithm is $\mathcal{O}\big(rn_2n_3(r+n_1+n_2+n_3)+n_2log(n_2)(n_1r+n_3r+n_1n_3)\big)$.

5. EXPERIMENTS

To verify the effectiveness of the proposed BLTNN-based restoration method, we conduct experiments on a sub-image cropped from Washington DC Mall (WDC) dataset with size $256 \times 256 \times 191$. For comprehensive evaluation, four representative denoising methods are selected, including LRMR [2], LRTR [5], NGmeet [10], and 3DTNN [6]. We choose the peak signal to noise ratio (PSNR ↑), the structural similarity (SSIM ↑), and the spectral angle mapping (SAM ↓) as quality metrics. The noisy data are simulated as follows:

Cases 1-2: Zero-mean Gaussian noise is added to all bands, where the standard deviation of the noise is randomly selected from [0.05, 0.15] and [0.1, 0.2], respectively.

Cases 3-4: Based on **Cases 1-2**, salt-and-pepper noise is added to each band, where the percentage of the noise is randomly selected from [0.1, 0.3].

Case 5: Based on **Case 4**, 10 bands are randomly selected to add stripes and the percentage of stripes is 5% in each band.

Table 1 presents the PSNR, SSIM, SAM, and average running time for the restoration of the WDC dataset using various methods. It is evident that the proposed BLTNN-based denoising method outperforms the compared methods for all metrics and requires less computational time. Visual representations of the recovered results are shown in Fig. 2. From Fig. 2, it is clear that our method effectively eliminates mixed noise while preserving the underlying structure. LRTR and

Table 1. The quantitative assessment of different methods on the WDC dataset. Best results are in boldface.

Case	Noisy image			LRMR			LRTR			NGmeet			3DTNN			BLTNN		
	PSNR	SSIM	SAM	PSNR	SSIM	SAM	PSNR	SSIM	SAM	PSNR	SSIM	SAM	PSNR	SSIM	SAM	PSNR	SSIM	SAM
Case 1	20.18	0.414	32.13	34.82	0.937	6.521	32.66	0.917	8.319	36.39	0.956	5.181	35.79	0.965	3.865	**37.05**	**0.971**	**3.769**
Case 2	16.67	0.267	40.85	32.34	0.900	8.441	29.94	0.873	9.728	34.09	0.938	5.332	33.33	0.946	4.928	**34.59**	**0.958**	**4.839**
Case 3	11.07	0.112	49.15	31.03	0.894	9.073	29.79	0.863	9.870	23.02	0.805	12.16	32.90	0.930	5.915	**34.68**	**0.942**	**5.346**
Case 4	10.27	0.089	51.23	29.26	0.856	10.71	27.99	0.829	11.56	22.90	0.797	11.92	29.75	0.865	8.334	**31.94**	**0.902**	**7.183**
Case 5	10.29	0.091	51.37	29.20	0.855	10.79	27.82	0.825	11.55	23.13	0.805	12.16	29.58	0.883	7.678	**31.82**	**0.899**	**7.227**
Average time(s)	–			185.1			40.8			42.7			179.9			**28.3**		

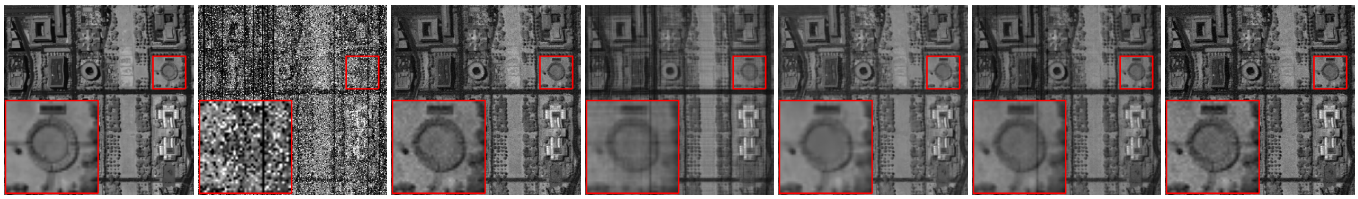

Clean image | Noisy image | LRMR [2] | LRTR [5] | NGmeet [10] | 3DTNN [6] | Proposed BLTNN

Fig. 2. Restoration results by different methods of the 67-th band of WDC dataset under Case 5.

3DTNN struggle to adequately remove mixed noise, while LRMR and NGmeet face challenges in accurately restoring local details.

6. CONCLUSION

This paper suggested a novel BLTD to comprehensively characterize the low-rank structure of HSIs. Based on BLTD, we developed a BLTNN-based model for HSI denoising. Furthermore, we presented an efficient ADMM-based algorithm to address this model. Experimental results demonstrated the superiority of the proposed method both quantitatively and qualitatively.

7. REFERENCES

[1] J. M. Bioucas-Dias, A. Plaza, N. Dobigeon, M. Parente, Q. Du, P. Gader, and J. Chanussot, "Hyperspectral unmixing overview: Geometrical, statistical, and sparse regression-based approaches," *IEEE J. Sel. Top. Appl. Earth Obs. Remote Sens.*, vol. 5, no. 2, pp. 354–379, 2012.

[2] H. Zhang, W. He, L. Zhang, H. Shen, and Q. Yuan, "Hyperspectral image restoration using low-rank matrix recovery," *IEEE Trans. Geosci. Remote Sens.*, vol. 52, no. 8, pp. 4729–4743, 2013.

[3] W. He, H. Zhang, L. Zhang, and H. Shen, "Hyperspectral image denoising via noise-adjusted iterative low-rank matrix approximation," *IEEE J. Sel. Top. Appl. Earth Obs. Remote Sens.*, vol. 8, no. 6, pp. 3050–3061, 2015.

[4] N. Renard, S. Bourennane, and J. Blanc-Talon, "Denoising and dimensionality reduction using multilinear tools for hyperspectral images," *IEEE Geosci. Remote Sens. Lett.*, vol. 5, no. 2, pp. 138–142, 2008.

[5] H. Fan, Y. Chen, Y. Guo, H. Zhang, and G. Kuang, "Hyperspectral image restoration using low-rank tensor recovery," *IEEE J. Sel. Top. Appl. Earth Obs. Remote Sens.*, vol. 10, no. 10, pp. 4589–4604, 2017.

[6] Y.-B. Zheng, T.-Z. Huang, X.-L. Zhao, T.-X. Jiang, and J. Huang, "Hyperspectral image denoising via convex low-fibered-rank regularization," in *Proc. IEEE Int. Geosci. Remote Sens. Symp.*, 2019, pp. 222–225.

[7] S. Boyd, N. Parikh, E. Chu, B. Peleato, and J. Eckstein, "Distributed optimization and statistical learning via the alternating direction method of multipliers," *Found. Trends Mach. Learn.*, vol. 3, no. 1, pp. 1–122, 2011.

[8] Q. Zhao, G. Zhou, S. Xie, L. Zhang, and A. Cichocki, "Tensor ring decomposition," *arXiv preprint arXiv:1606.05535*, 2016.

[9] J. Yu, C. Li, Q. Zhao, and G. Zhao, "Tensor-ring nuclear norm minimization and application for visual: Data completion," in *Proc. IEEE Int. Conf. Acoust. Speech Signal Process.*, 2019, pp. 3142–3146.

[10] W. He, Q. Yao, C. Li, N. Yokoya, and Q. Zhao, "Non-local meets global: An integrated paradigm for hyperspectral denoising," in *Proc. IEEE Conf. Comput. Vis. Pattern Recognit.*, 2019, pp. 6868–6877.